

# Probing the dynamical behavior of dark energy

Rong-Gen Cai,<sup>\*</sup> Qiping Su,<sup>†</sup> and Hong-Bo Zhang<sup>‡</sup>

*Key Laboratory of Frontiers in Theoretical Physics,  
Institute of Theoretical Physics, Chinese Academy of Sciences,  
P.O. Box 2735, Beijing 100190, China*

## Abstract

We investigate dynamical behavior of the equation of state of dark energy  $w_{de}$  by employing the linear-spline method in the region of low redshifts from observational data (SnIa, BAO, CMB and 12  $H(z)$  data). The redshift is binned and  $w_{de}$  is approximated by a linear expansion of redshift in each bin. We leave the divided points of redshift bins as free parameters of the model, the best-fitted values of divided points will represent the turning positions of  $w_{de}$  where  $w_{de}$  changes its evolving direction significantly (if there exist such turnings in our considered region). These turning points are natural divided points of redshift bins, and  $w_{de}$  between two nearby divided points can be well approximated by a linear expansion of redshift. We find two turning points of  $w_{de}$  in  $z \in (0, 1.8)$  and one turning point in  $z \in (0, 0.9)$ , and  $w_{de}(z)$  could be oscillating around  $w = -1$ . Moreover, we find that there is a  $2\sigma$  deviation of  $w_{de}$  from  $-1$  around  $z = 0.9$  in both correlated and uncorrelated estimates.

---

<sup>\*</sup>Electronic address: cairg@itp.ac.cn

<sup>†</sup>Electronic address: sqp@itp.ac.cn

<sup>‡</sup>Electronic address: hbzhang@itp.ac.cn

## I. INTRODUCTION

It has been more than ten years since our universe was found to be in accelerating expansion [1]. A dominated and uniformly distributed energy component of the universe, called dark energy (DE), should be responsible for the acceleration. Many DE models have been proposed [2–6]. The simplest cosmological model is  $\Lambda$ CDM model, which contains a cosmological constant as dark energy. While  $\Lambda$ CDM model is still consistent well with all observational data, a lot of efforts have been made to find out whether DE is time-evolving or is just the cosmological constant. To do that, several parameterizations of equation of state (EoS) of DE have been proposed to fit with observational data, such as the ansatz  $w_{de} = w_0 + w'z$  [7], the EoS expanded by redshift, and the CPL parametrization [8, 9]  $w_{de} = w_0 + w_a z / (1 + z)$ , expanded by scale factor. Both of them contain two free parameters:  $w_0$ , the present value of EoS, and  $w'$  or  $w_a$ , represents the time evolution of EoS. Clearly, constraints of EoS obtained by using these parameterizations are model-dependent. Given an unreal assumption of EoS of DE, one may lead to wrong conclusions. Some model-independent methods have also been proposed [10–13], such as the widely-used uncorrelated bandpower estimates (UBE) [11, 14], in which the redshift is binned and  $w_{de}$  is assumed as a constant in each redshift bin. Note that the UBE method just approximates the actual  $w_{de}$  by an averaged constant in each bin if DE is dynamical. If there are sufficient data,  $w_{de}(z)$  can be accurately reconstructed. However, current data could only support a few bins, thus UBE is always used to test the deviation of  $w_{de}$  from the cosmological constant and used as a supplementary for the parameterizations of  $w_{de}$ . Note that the cubic-spline interpolation has also been proposed to study the binned  $w_{de}(z)$  [15, 16]. However, no convincing evidence of dynamic DE has been found [15–17]. In addition, let us note that the ansatz,  $w_{de} = w_0 + w'z$ , of redshift expansion and CPL parametrization exclude the possibility of an oscillation EoS, if they are used to fit the whole expansion history of the universe. While the UBE method needs enough bins to reveal the real dynamical behavior of DE, the errors will get larger as the number of bins increases.

In this paper, we would like to probe the dynamical behavior of  $w_{de}$  by using the linear-spline method. We will approximate  $w_{de}$  in each redshift bin by a linear function  $w = w_0 + w'z$ , and require that  $w_{de}(z)$  is continuous in the region under consideration. Since most of data we used (e.g., SnIa data) are in low redshift, we will focus on the region of low

redshift, such as  $z \in (0, 0.9)$  and  $z \in (0, 1.8)$ . In such regions, the width of each redshift bin is small and the linear expansion could be a better approximation of  $w_{de}(z)$  than a constant in each bin. When fitting with the observational data, we leave the divided positions of bins  $z_i$  as free parameters. Since the linear function is monotonic, the best-fitted  $z_i$  can represent the turning points of  $w_{de}(z)$ , where  $w_{de}(z)$  is not linear enough or even non-monotonic (i.e., where  $d^2w_{de}/dz^2$  departs from zero substantially). Actually we do find some turning points of  $w_{de}$  from observational data, and the constructed  $w_{de}(z)$  just turns its evolution direction at the best-fitted positions of  $z_i$ . In this way, we only need to divide redshift into a few bins, the turning points are natural divided points of redshift and  $w_{de}$  between two nearby points can be accurately reconstructed by linear expansion. Compared to the cubic-spline method, the linear-spline (LS) method can find turning locations of  $w_{de}$  more accurately and reduce the errors due to less the number of bins. The LS method is also nearly model-independent, like the piecewise constant and cubic-spline method. Replacing the linear expansion by CPL parametrization in each bin, we have reached the almost same results.

For the current status of observational data, LS method may be more suitable to study  $w_{de}$  than the piecewise constant and the cubic spline method. If DE is dynamical or even oscillating, by using the LS method it should be more possible to find deviations from the cosmological constant, at the turning points the deviation from  $-1$  should be more explicit. If DE is just the cosmological constant, it seems more confident if the best-fitted linear expansions construct an  $w = -1$  line, while the oscillation of  $w_{de}$  around  $w = -1$  could disappear by averaging with the piecewise constant method. Compared to the piecewise constant case, the only price we pay is that there is one more parameter in the LS method if the number of bins is the same in two cases. Compared to the cubic spline method, the form of  $w_{de}(z)$  in each bin only depends on values of  $w_{de}$  at two boundaries, thus the parameters in  $w_{de}(z)$  will not be heavily correlated. Furthermore, the cubic-spline method seems not suitable for finding the turning points of  $w_{de}$ . In all, the LS method could reconstruct  $w_{de}$  explicitly by using the least number of bins, and errors of the parameters from observational data will be small, compared to the case with more bins.

The paper is organized as follows. In section II we introduce in detail the method we will use and construct corresponding cosmological models. In section III, we show how to fit our model with 397 Constitution SnIa sample [18], BAO data from SDSS DR7 [19], CMB datapoints  $(R, l_a, z_*)$  from WMAP5 [20] and 12 Hubble evolution data [21, 22]. The fitting

results are presented in section IV. We give our conclusions and discussions in section V.

## II. METHODOLOGY

To fit models with observational data, we need to know the form of Hubble function  $H(z)$  (or  $E(z) = H(z)/H_0$ ). In a flat FRW universe

$$E^2(z) = \Omega_r^{(0)}(1+z)^4 + \Omega_b^{(0)}(1+z)^3 + \Omega_{dm}^{(0)}(1+z)^3 + \Omega_{de}^{(0)}F(z), \quad (1)$$

where  $\Omega_r^{(0)}$ ,  $\Omega_b^{(0)}$ ,  $\Omega_{dm}^{(0)}$  and  $\Omega_{de}^{(0)}$  are present values of the dimensionless energy density for radiations, baryons, dark matter and dark energy, respectively, and  $\Omega_r^{(0)} + \Omega_b^{(0)} + \Omega_{dm}^{(0)} + \Omega_{de}^{(0)} = 1$ . The energy densities of baryons and dark matter are always written together as  $\Omega_b^{(0)}(1+z)^3 + \Omega_{dm}^{(0)}(1+z)^3 = \Omega_m^{(0)}(1+z)^3$ . The radiation density is the sum of photons and relativistic neutrinos [20]:

$$\Omega_r^{(0)} = \Omega_\gamma^{(0)}(1 + 0.2271N_n),$$

where  $N_n$  is the number of neutrino species and  $\Omega_\gamma^{(0)} = 2.469 \times 10^{-5}h^{-2}$  for  $T_{cmb} = 2.725K$  ( $h = H_0/100 \text{ Mpc} \cdot \text{km} \cdot \text{s}^{-1}$ ). The evolving function  $F(z)$  for DE depends on  $w_{de}(z)$ :

$$F(z) = e^{3 \int_0^z \frac{1+w_{de}}{1+x} dx}. \quad (2)$$

For example,

$$F(z) = (1+z)^{3(1+w_0+w_a)} e^{-\frac{3w_a z}{1+z}},$$

for the CPL parametrization and  $F(z) = 1$  for  $w_{de} = -1$ , respectively. Here we divide  $z \in (0, \infty)$  into  $m+1$  bins and assume  $w_{de}(z)$  in the first  $m$  bins as

$$w_{de}(z_{n-1} < z \leq z_n) = w_{n-1} + w'_n \times (z - z_{n-1}), \quad (1 \leq n \leq m) \quad (3)$$

and require  $w_{de}(z)$  to be continuous at divided points:

$$w_n = w_{n-1} + w'_n \times (z_n - z_{n-1}), \quad (1 \leq n \leq m-1) \quad (4)$$

Note that here prime does not represent a derivative, instead  $w'_n$  is just the slope of the linear expansion in the  $n^{\text{th}}$  bin. Thus the independent parameters are

$$w_0, w'_1, w'_2, \dots, w'_n, \dots, w'_m \quad (5)$$

where the total number of parameters is  $1 + m$  with  $m \geq 1$ . Alternatively, we can express  $w_{de}$  as

$$w_{de}(z_{n-1} < z \leq z_n) = w(z_{n-1}) + \frac{w(z_n) - w(z_{n-1})}{z_n - z_{n-1}}(z - z_{n-1}), \quad (1 \leq n \leq m) \quad (6)$$

Now the parameters become  $w(z_n)$ 's, which are values of  $w_{de}$  at the divided points and boundaries  $z_n$  ( $0 \leq n \leq m$ ). In this case we have

$$F(z_{n-1} < z \leq z_n) = e^{3\{[w(z_{n-1}) - w(0)] + \frac{w(z_n) - w(z_{n-1})}{z_n - z_{n-1}}(z - z_{n-1})\}} \left( \frac{1 + z}{1 + z_{n-1}} \right)^{3 \frac{w(z_{n-1})(1+z_n) - w(z_n)(1+z_{n-1})}{z_n - z_{n-1}}} \\ \times (1 + z)^3 \prod_{i=1}^{n-1} \left( \frac{1 + z_i}{1 + z_{i-1}} \right)^{3 \frac{w(z_{i-1})(1+z_i) - w(z_i)(1+z_{i-1})}{z_i - z_{i-1}}}, \quad (1 \leq n \leq m) \quad (7)$$

where we have used  $z_0 = 0$ . For  $w_{de}$  in the last bin  $z \in (z_m, \infty)$ , we set it to be a constant  $w_L$ , and

$$F(z > z_m) = F(z_m) \left( \frac{1 + z}{1 + z_m} \right)^{3(1+w_L)} \quad (8)$$

Now the formula for  $H(z)$  is ready.

There is one more thing to be mentioned: once we have fitted our model with the data introduced in the next section, errors of  $w(z_i)$  are correlated, i.e., the errors of  $w(z_i)$  are dependent on each other. New parameters can be defined by transforming the covariance matrix of  $w(z_i)$ , so that errors of new parameters are decorrelated and do not entangle with each other. The new uncorrelated parameters are referred to as the principal components [10, 23], and they are directly related to their own locations (unlike the correlated case). So errors of the uncorrelated parameters are more interpretable and meaningful. For more discussions and implications of the uncorrelated parameters, we refer to the references [11, 14, 24]. In section IV, we will show both errors of correlated and uncorrelated parameters of  $w_{de}$ . The uncorrelated technique we adopt from [11] is as follows.

1. Get the covariance matrix

$$C = \langle WW^T \rangle - \langle W \rangle \langle W^T \rangle \quad (9)$$

where  $W$  is the vector of  $w(z_i)$ . The Fisher matrix  $F$  is defined by  $F = C^{-1}$ .

2. Diagonalize the Fisher matrix by an orthogonal matrix  $O$

$$F = O^T \Lambda O, \quad (10)$$

where  $\Lambda$  is diagonal.

3. Define a new matrix  $U$  as

$$U = O^T \Lambda^{1/2} O, \quad (11)$$

and normalize  $U$  so that the sum of its each row is equal to 1.

4. Define new parameters  $q_i$  by  $q = UW$ , where  $q_i$  are components of the vector  $q$ .

Clearly for the case of  $w(z) = -1$  (i.e., the cosmological constant case), we will have  $q_i = -1$ . The covariance of new parameters is

$$\langle (q_i - \langle q_i \rangle)(q_j - \langle q_j \rangle) \rangle = \frac{\delta_{ij}}{\sum_a (F^{1/2})_{ia} \sum_b (F^{1/2})_{jb}}. \quad (12)$$

In this way the errors of the new parameters  $q_i$  become uncorrelated.

The uncorrelated parameters  $q_i$  are linear combinations of  $w(z_i)$ , and the coefficients are just row elements of  $U$ . The transformation matrix  $U$  constructed in this method ensures that most of the coefficients are positive. So most of coefficients are in  $(0, 1)$ . In this way, the original correlated parameters are weight-averaged, which leads to the uncorrelated parameters  $q_i$ . As a result, if  $w_{de}$  is of the quintom form, the uncorrelated  $w_{de}$  always looks more consistent with the cosmological constant than the correlated one.

### III. SETS OF OBSERVATIONAL DATA

We will fit our model by employing some observational data including SnIa, BAO, CMB and Hubble evolution data. The data for SnIa are the 397 Constitution sample [18].  $\chi_{sn}^2$  for SnIa is obtained by comparing theoretical distance modulus  $\mu_{th}(z) = 5 \log_{10}[(1+z) \int_0^z dx/E(x)] + \mu_0$  ( $\mu_0 = 42.384 - 5 \log_{10} h$ ) with observed  $\mu_{ob}$  of supernovae:

$$\chi_{sn}^2 = \sum_i^{397} \frac{[\mu_{th}(z_i) - \mu_{ob}(z_i)]^2}{\sigma^2(z_i)} \quad (13)$$

To reduce the effect of  $\mu_0$ , we expand  $\chi_{sn}^2$  with respect to  $\mu_0$  [25]:

$$\chi_{sn}^2 = A + 2B\mu_0 + C\mu_0^2 \quad (14)$$

where

$$A = \sum_i \frac{[\mu_{th}(z_i; \mu_0 = 0) - \mu_{ob}(z_i)]^2}{\sigma^2(z_i)},$$

$$B = \sum_i \frac{\mu_{th}(z_i; \mu_0 = 0) - \mu_{ob}(z_i)}{\sigma^2(z_i)}, \quad C = \sum_i \frac{1}{\sigma^2(z_i)} \quad (15)$$

Eq. (14) has a minimum as

$$\tilde{\chi}_{sn}^2 = \chi_{sn,min}^2 = A - B^2/C$$

which is independent of  $\mu_0$ . In fact, it is equivalent to performing an uniform marginalization over  $\mu_0$ , the difference between  $\tilde{\chi}_{sn}^2$  and the marginalized  $\chi_{sn}^2$  is just a constant [25]. We will adopt  $\tilde{\chi}_{sn}^2$  as the chi-square between theoretical model and SnIa data.

We will also use the Baryon Acoustic Oscillations (BAO) data from SDSS DR7 [19], the datapoints are

$$\frac{r_s(z_d)}{D_V(0.275)} = 0.1390 \pm 0.0037 \quad (16)$$

and

$$\frac{D_V(0.35)}{D_V(0.2)} = 1.736 \pm 0.065 \quad (17)$$

where  $r_s(z_d)$  is the comoving sound horizon at the baryon drag epoch [26], and

$$D_V(z) = \left[ \left( \int_0^z \frac{dx}{H(x)} \right)^2 \frac{z}{H(z)} \right]^{1/3} \quad (18)$$

encodes the visual distortion of a spherical object due to the non Euclidianity of a FRW space-time.

The CMB datapoints we will use are  $(R, l_a, z_*)$  from WMAP5 [20].  $z_*$  is the redshift of recombination [28],  $R$  is the scaled distance to recombination

$$R = \sqrt{\Omega_m^{(0)}} \int_0^{z_*} \frac{dz}{E(z)}, \quad (19)$$

and  $l_a$  is the angular scale of the sound horizon at recombination

$$l_a = \pi \frac{r(a_*)}{r_s(a_*)}, \quad (20)$$

where  $r(z) = \int_0^z dx/H(x)$  is the comoving distance and  $r_s(a_*)$  is the comoving sound horizon at recombination

$$r_s(a_*) = \int_0^{a_*} \frac{c_s(a)}{a^2 H(a)} da, \quad a_* = \frac{1}{1 + z_*} \quad (21)$$

where the sound speed  $c_s(a) = 1/\sqrt{3(1 + \bar{R}_b a)}$  and  $\bar{R}_b = 3\Omega_b^{(0)}/4\Omega_\gamma^{(0)}$  is the photon-baryon energy density ratio.

The  $\chi^2$  of the CMB data is constructed as:

$$\chi_{cmb}^2 = X^T C_M^{-1} X \quad (22)$$

where

$$X = \begin{pmatrix} l_a - 302.1 \\ R - 1.71 \\ z_* - 1090.04 \end{pmatrix} \quad (23)$$

and the inverse covariance matrix

$$C_M^{-1} = \begin{pmatrix} 1.8 & 27.968 & -1.103 \\ 27.968 & 5667.577 & -92.263 \\ -1.103 & -92.263 & 2.923 \end{pmatrix} \quad (24)$$

The fourth set of observational data is 12 Hubble evolution data from [21] and [22], its  $\chi_H^2$  is defined as

$$\chi_H^2 = \sum_{i=1}^{12} \frac{[H(z_i) - H_{ob}(z_i)]^2}{\sigma_i^2}. \quad (25)$$

Note that redshifts of these data fall in the region  $z \in (0, 1.75)$ .

In summary,

$$\chi_{total}^2 = \tilde{\chi}_{sn}^2 + \chi_{cmb}^2 + \chi_{bao}^2 + \chi_H^2. \quad (26)$$

## IV. FITTING RESULTS

### A. Model I

At first, we divide the whole region of redshift into 4 bins (i.e.,  $m = 3$ ), the divided points and boundaries are  $(0, z_1, z_2, 1.8, \infty)$ , where  $z_1$  and  $z_2$  are left as free parameters of the model, and  $0 < z_1 < z_2 < 1.8$ . In the fourth bin we set  $w_L = -1$ . It means that we divide the region with  $z \in (0, 1.8)$  into 3 bins and seek for two possible turning points of  $w_{de}(z)$  in this region. The reconstructed  $w_{de}$  of the best-fitted model is shown in Fig. 1,

Models	$\tilde{\chi}_{sn,min}^2$	$\chi_{cmb,min}^2$	$\chi_{bao,min}^2$	$\chi_{H,min}^2$	$\chi_{total,min}^2$
Model I	459.728	0.204	1.494	5.983	467.409
CPL	465.621	0.251	1.716	10.818	478.406
$\Lambda$ CDM	465.759	1.014	1.470	10.850	479.093

TABLE I: The best-fitted  $\chi^2$  of four data sets for Model I, CPL model and the  $\Lambda$ CDM model.



which indicates that there exist (at least) two turning points of  $w_{de}$  in  $z \in (0, 1.8)$  and the best-fitted values  $z_1 = 0.44$  and  $z_2 = 1.07$ . Here  $\chi_{total,min}^2 = 467.409$  for the best-fitted parameters, roughly speaking it is a good improvement, compared with the corresponding  $\chi_{total,min}^2 = 478.406$  for the best-fitted CPL model and  $\chi_{total,min}^2 = 479.093$  for the  $\Lambda$ CDM model. As shown in Table I, this improvement of  $\chi_{total,min}^2$  is mainly due to the decrease of  $\tilde{\chi}_{sn,min}^2$  and  $\chi_{H,min}^2$ . It is not surprising, as redshifts of the two data sets are distributed in whole range of  $z \in (0, 1.8)$ , while the BAO data are in the region  $z \leq 0.35$  and the CMB data are in the region  $z \in (0, z_* \sim 1090)$ . The result implies that these two data sets are quite favor of turnings of  $w_{de}$  around  $z = 0.44$  and  $z = 1.07$  respectively. This result is consistent with recent UBE of  $w_{de}$  [27]. While in CPL and  $\Lambda$ CDM models it is impossible to have such turnings of  $w_{de}$ , which leads to the big differences between  $\chi_{total,min}^2$  of Model I and that of  $\Lambda$ CDM and CPL models. This result also implies that there exists the possibility with an oscillating EoS. Note that the error bar of  $w_{de}$  in the third bin is larger than those in the first two bins because there are much less data points.

We have also divided the region of  $z \in (0, 1.8)$  into 4 bins, and found that there is almost

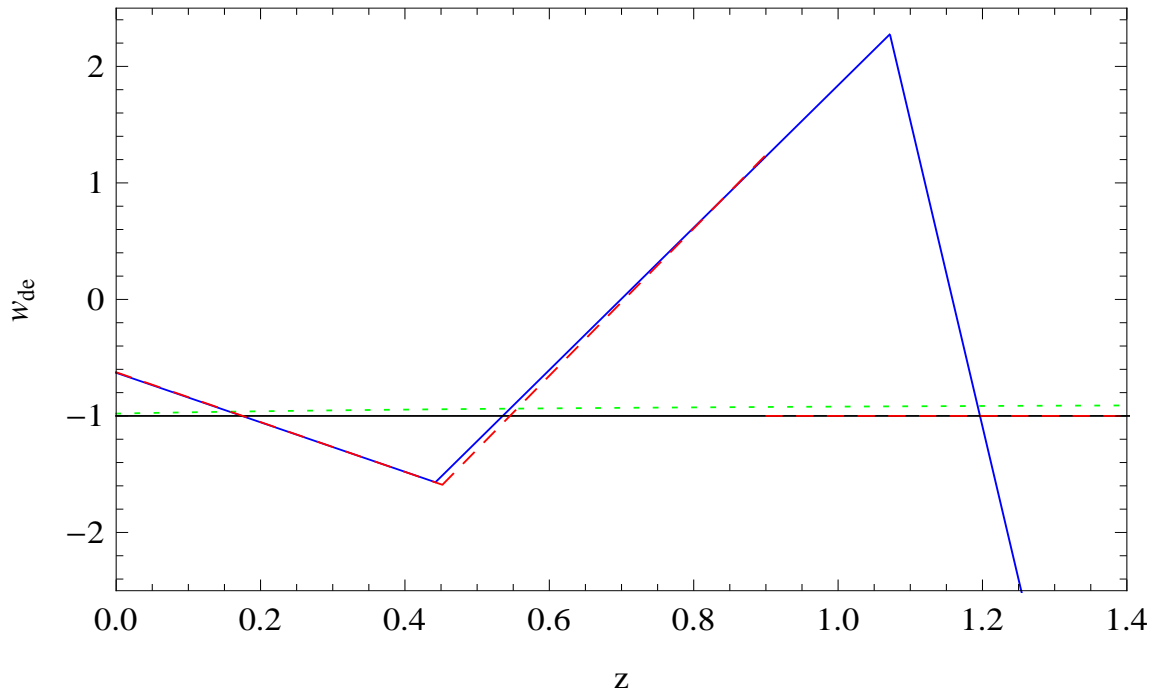


FIG. 1: The best-fitted  $w_{de}$  for Model I (blue, solid), Model II (red, dashed) and the CPL model (green, dotted), the black line is for  $w = -1$ .

no improvement of  $\chi_{total,min}^2$  compared to the case of 3 bins, which indicates there is no more turning points of  $w_{de}$  in this region.

TABLE II: The best-fitted parameters for Model I.

parameters	$h$	$\Omega_b^{(0)}$	$\Omega_m^{(0)}$	$z_1$	$z_2$	$w(0)$	$w(z_1)$	$w(z_2)$	$w(1.8)$	$w_L$
best-fitted values	0.688	0.049	0.279	0.44	1.07	-0.63	-1.57	2.28	-16.84	{-1}

## B. Model II

As data points with  $z > 1$  are rather less than those with  $z < 1$ , to see clearly the evolution behavior of EoS in the region of low redshift, we now focus on the region with  $z \in (0, 0.9)$ , avoiding the possible turning point around  $z = 1$ , and set the divided points as:  $(0, z_1, 0.9, \infty)$ , i.e.,

$$w_{de}(z) = \begin{cases} w(0) + \frac{w(z_1)-w(0)}{z_1}z, & 0 < z \leq z_1 \\ w(z_1) + \frac{w(0.9)-w(z_1)}{0.9-z_1}(z-z_1), & z_1 < z \leq 0.9 \\ -1, & 0.9 < z < \infty \end{cases} \quad (27)$$

In this case, we obtain the best-fitted tuning point  $z_1 = 0.45$ , and the best-fitted  $w_{de}(z)$  is shown in Fig. 1 (the red, dashed line) which almost coincides with the best-fitted  $w_{de}(z)$  of Model I in  $z \in (0, 0.9)$ . This indicates that the data favor  $w_{de}(z)$  to turn its evolution direction around  $z = 0.45$ , and favor an EoS with crossing the cosmological constant ( $w = -1$ ) [29]. Then we obtain  $1\sigma$  and  $2\sigma$  errors of parameters by using the MCMC method. Here we have fixed  $z_1 = 0.45$  in the process to obtain the errors of the parameters. Note that the errors of the parameters  $w_{de}(z_i)$  also represent errors of whole  $w_{de}(z)$  in each bin, the  $1\sigma$  and  $2\sigma$  errors of  $w_{de}(z)$  shown in Fig. 2 are obtained by connecting the corresponding error ranges of  $w_{de}(z_i)$ . If another parameter set of  $w_{de}(z)$  (as introduced in section II) was used, one will get the same result as that of Fig. 2.

We see from the top left panel of Fig. 2 that there are deviations of  $w_{de}$  from  $-1$  around  $z = 0$  and  $z = 0.45$  beyond  $1\sigma$ , and around  $z = 0.9$  the deviation is beyond  $2\sigma$ . We decorrelate the parameters in  $w_{de}(z)$  by using the technique introduced in section II. The uncorrelated errors are shown in the bottom left panel of Fig. 2. In that case, there are no

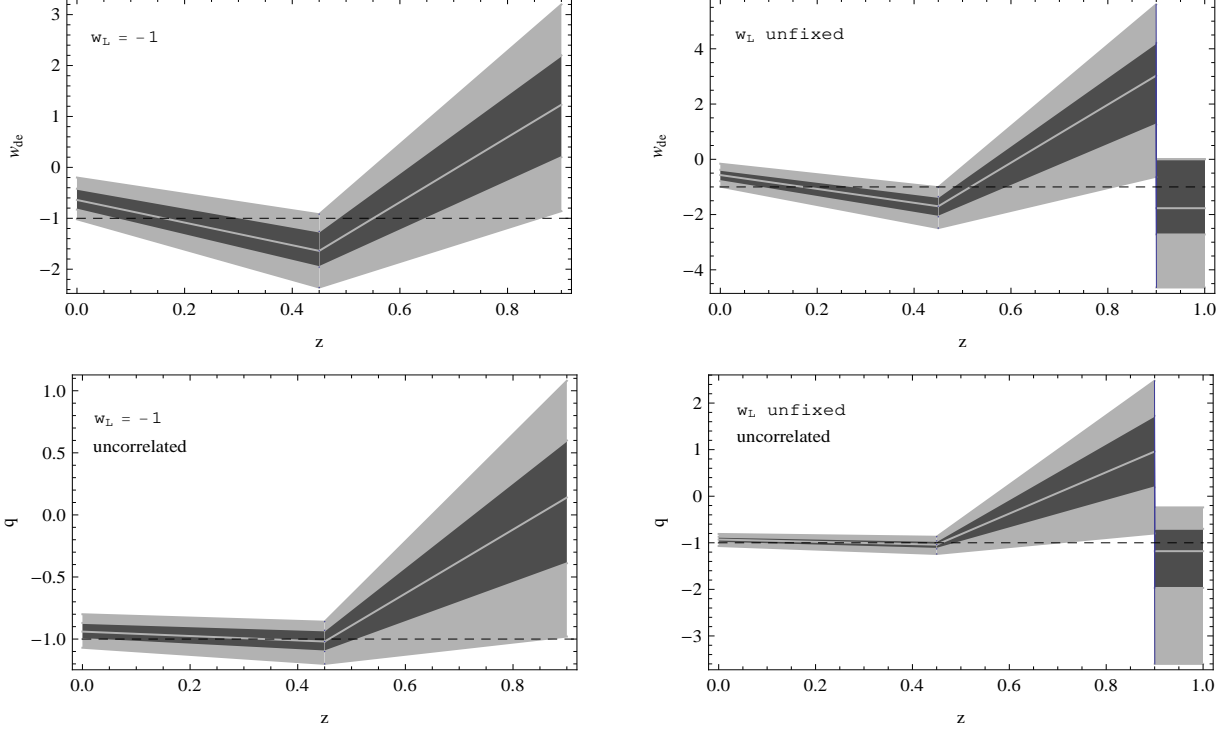


FIG. 2:  $1\sigma$  and  $2\sigma$  errors of  $w_{de}$  in Model II. Left panels are for the model with  $w_L = -1$  and right panels are with  $w_L$  floating, top panels are for correlated parameters in  $w_{de}(z)$  and the bottom panels are for uncorrelated ones.

more explicit deviations from  $-1$  around  $z = 0$  and  $z = 0.45$ , however, there is still a  $2\sigma$  deviation from  $-1$  around  $z = 0.9$ .

One may suspect that the explicit derivations are caused due to the fact that we have fixed the value of  $w_{de}$  as  $w_L = -1$  in the third bin. To check this, we consider the case with a floating  $w_L$ . Two right panels of Fig. 2 show the correlated and uncorrelated results for the case with the floating  $w_L$ . We see that in this case, there is even larger deviation from  $-1$  around  $z = 0.9$ . We have also used the CPL parametrization to replace the linear expansion in each bin, and found that the errors are almost the same as those in the case of the linear expansion and there is still a deviation of  $w_{de}$  from  $-1$  around  $z = 0.9$ . We will extend our discussion of this result in the last section. In Fig. 3 we plot the likelihoods and weight functions of the uncorrelated parameters  $q_i$ . The weight functions are constructed from the transformation matrix  $U$ , which show how uncorrelated parameters  $q_i$  are determined. It is shown that the parameters of  $w_{de}$  are less correlated than that of the cubic-spline case [16].

We have also divided  $z \in (0, 0.9)$  into three bins, to see whether there exist two turning

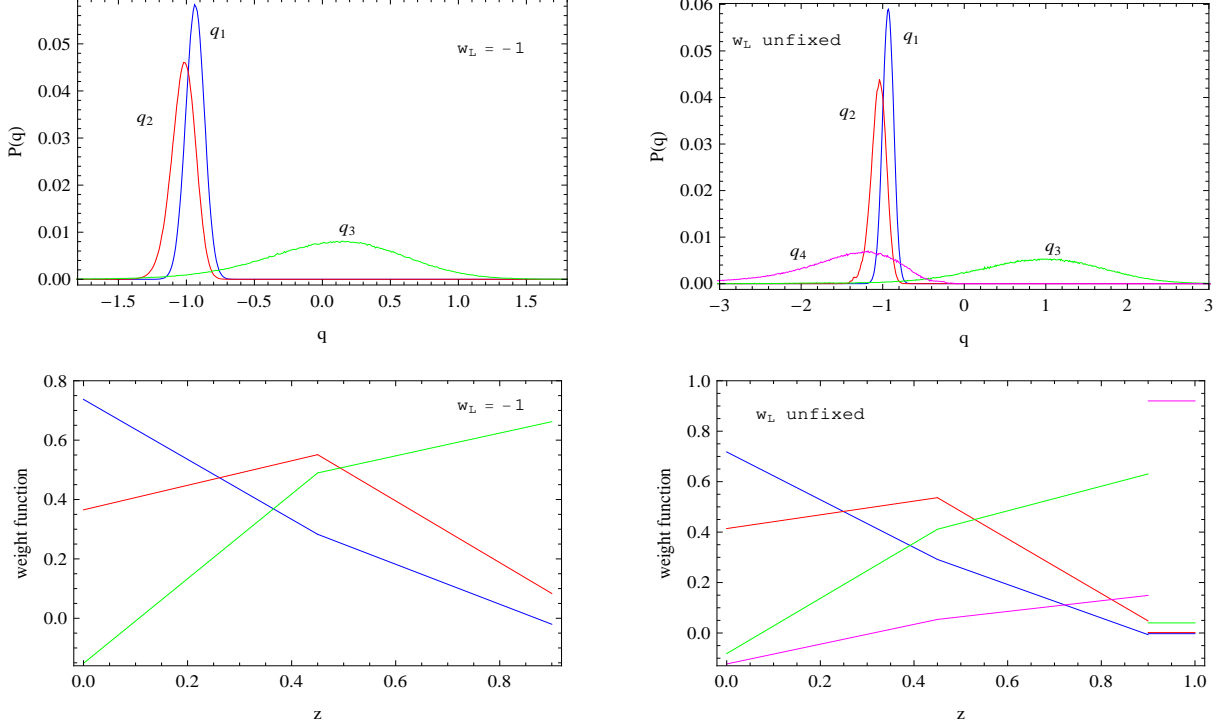


FIG. 3: Likelihoods and weight functions of uncorrelated parameters  $q_i$  and corresponding weight functions. The left panels are for the model with  $w_L = -1$  and the right panels are for the case with a floating  $w_L$ .

TABLE III: The best-fitted parameters and  $2\sigma$  errors for Model II with  $w_L$  fixed to  $-1$  or floating. ML is for “Maximum Likelihood”, and the value in  $\{\}$  means this parameter has been fixed.

parameters	$h$	$\Omega_b^{(0)}$	$\Omega_m^{(0)}$	$z_1$	$w(0)$	$w(z_1)$	$w(0.9)$	$w_L$
best-fitted values	0.684	0.050	0.282	0.45	-0.63	-1.59	1.24	$\{-1\}$
ML and $2\sigma$ errors	$0.684^{+0.025}_{-0.026}$	$0.050^{+0.004}_{-0.003}$	$0.286^{+0.03}_{-0.03}$	$\{0.45\}$	$-0.64^{+0.44}_{-0.38}$	$-1.64^{+0.72}_{-0.72}$	$1.23^{+1.97}_{-2.09}$	$\{-1\}$
best-fitted values	0.687	0.049	0.280	$\{0.45\}$	-0.59	-1.69	2.54	-1.72
ML and $2\sigma$ errors	$0.687^{+0.027}_{-0.026}$	$0.049^{+0.004}_{-0.004}$	$0.285^{+0.033}_{-0.030}$	$\{0.45\}$	$-0.57^{+0.41}_{-0.42}$	$-1.70^{+0.69}_{-0.79}$	$3.03^{+2.58}_{-3.66}$	$-1.77^{+1.78}_{-2.87}$

points of  $w_{de}$  in this region. We found that with the additional 2 parameters ( $z_2$  and  $w(z_2)$ ), there is almost no improvement of  $\chi_{min}^2$ , compared to the 2 bins case (Model II). This indicates that there is no more turning points and  $w_{de}(z)$  can be well approximated by just two linear expansions in the region  $z \in (0, 0.9)$ . Of course, there is another possibility that the current data are not enough to find out more turning points.

## V. CONCLUSIONS AND DISCUSSIONS

In this paper we have investigated the dynamical behavior of the EoS of DE in the region of low redshift in a nearly model-independent way. The redshift in that region is binned and  $w_{de}$  in each bin is approximated by a linear expansion of redshift  $z$ , and in the large redshift region we set  $w_{de}$  to be a constant  $w_L$ . While fitting the model with some observational data which include SNIa, BAO, CMB and Hubble evolution data, we leave the divided points of bins as free parameters. If the evolution of  $w_{de}$  is not monotonous, or is not linear enough in the region under consideration, the best-fitted divided points will represent the turning points, where  $w_{de}$  changes its evolving direction significantly. In this way we can explicitly reconstruct  $w_{de}$  by using a few bins, and the errors of parameters from observational data will be small due to the small number of bins. First we have tried to find the turning points within the region of redshift  $z \in (0, 1.8)$ , and set  $w_L = -1$  in the region  $z \in (1.8, \infty)$  (Model I). Our results show that the data favor two turning points of  $w_{de}$  in  $z \in (0, 1.8)$ , and  $w_{de}$  may have an oscillation form [30]. Our results are consistent with those by the UBE method in [27].

Since the main data points are in  $z \in (0, 1)$  and our result in Model I shows there may be a turning point around  $z \sim 1$ , to see clearly the dynamical behavior of EoS in that region, we have focused on the region  $z \in (0, 0.9)$  in Model II. We have found one turning point only in  $z \in (0, 0.9)$ , the reconstructed  $w_{de}$  in the best-fitted model is almost the same as that reconstructed in Model I in  $z \in (0, 0.9)$ . We have also obtained the errors of  $w_{de}$  at  $1\sigma$  and  $2\sigma$  in  $z \in (0, 0.9)$ . In both correlated and uncorrelated estimates with a fixed  $w_L = -1$  or a floating constant  $w_L$ , we found that there is a  $2\sigma$  deviation of  $w_{de}$  from  $-1$  around  $z = 0.9$ .

It is interesting to see whether the deviation of EoS from  $-1$  around  $z = 0.9$  is physical, or is caused by some unknown technical causes in fitting. If it is physical, it then clearly shows that DE is dynamical. But in UBE of  $w_{de}$  there seems no such distinct deviation around  $z = 0.9$ , it may be due to the difference between the discontinuity of  $w_{de}$  in the piecewise constant case and the continuity in LS case [31]. In [16], where the cubic-spline method is used, there is also no such an explicit deviation around  $z = 0.9$ , but it is likely due to its set of EoS in the last bin  $w_L = w(1)$ : to fit well with the data of  $z > 1$ ,  $w(1)$  should be much minus, which would suppress the reconstructed  $w_{de}$  around  $z = 1$ . Of course, it is also possible that such a big deviation around  $z = 0.9$  is due to the non-smoothness of

$w_{de}$  at the divided points in our LS method. In the LS method,  $w_{de}$  is continuous, but not smooth at the divided points, i.e., its derivative is not continuous at those points. In fact,  $w_{de}$  in LS method can be made smooth at the divided points, such as by the relation

$$w_{de}(z) = w_0 + \sum_{i=1}^m \frac{w'_i - w'_{i-1}}{2} \left( z + \Delta \ln \frac{\cosh(\frac{z-z_{i-1}}{\Delta})}{\cosh(z_{i-1}/\Delta)} \right), \quad (28)$$

where  $w'_i$  is the slope of linear expansion in the  $i^{th}$  bin ( $i \geq 1$  and  $w'_0 = 0$ ), and  $\Delta$  is related to the smoothed extent at the divided points. With this parameterization, one can still find out the turning positions of  $w_{de}$  that are favored by observational data, and perturbations of DE can be calculated.

Furthermore our results are also dependent on the data set we have used [32]. For example, although there is still a  $2\sigma$  deviation at  $z = 0.9$  by using the widely-used data set SnIa + CMB-shift R + BAO parameter A [33], now the best-fitted turning point in  $z \in (0, 0.9)$  changes to  $z = 0.39$ . Whatever, from the observational data we have used, a big deviation of  $w_{de}$  from  $-1$  around  $z = 0.9$  is found. Unlike the deviations around  $z = 0$  and  $z = 0.45$ , this deviation around  $z = 0.9$  does not to be reduced in the uncorrelated estimate. At least, our result shows that if DE is dynamical it is more possible to find the deviation of  $w_{de}$  from  $-1$  around this redshift value.

If the EoS of DE is indeed of an oscillating behavior around  $-1$ , it is then not surprising that the cosmological constant always fits well with observational data because the oscillating behavior could be smeared in the luminosity distance. However, if the oscillation region of  $w_{de}$  is wide enough (like the case of our best-fitted  $w_{de}$  in Model I), DE may be distinguished confidently from the cosmological constant by more precise astronomical observations in the next generation. In addition, let us mention that an oscillating behavior of  $w_{de}$  is also possibly due to some systematic errors in observational data, or due to some interactions between DE and dark matter [34].

## Acknowledgments

RGC thanks Y.G. Gong and B. Wang for some relevant discussions. This work was partially supported by NNSF of China (No. 10821504 and No. 10975168) and the National

- [1] A. G. Riess *et al.* [Supernova Search Team Collaboration], *Astron. J.* **116**, 1009 (1998) [arXiv:astro-ph/9805201]; S. Perlmutter *et al.* [Supernova Cosmology Project Collaboration], *Astrophys. J.* **517**, 565 (1999) [arXiv:astro-ph/9812133].
- [2] E. J. Copeland, M. Sami and S. Tsujikawa, *Int. J. Mod. Phys. D* **15**, 1753 (2006) [arXiv:hep-th/0603057].
- [3] R. R. Caldwell and P. J. Steinhardt, *Phys. Rev. D* **57**, 6057 (1998) [arXiv:astro-ph/9710062].
- [4] P. J. Steinhardt, L. M. Wang and I. Zlatev, *Phys. Rev. D* **59**, 123504 (1999) [arXiv:astro-ph/9812313].
- [5] S. Capozziello, S. Carloni and A. Troisi, *Recent Res. Dev. Astron. Astrophys.* **1**, 625 (2003) [arXiv:astro-ph/0303041].
- [6] M. Li, *Phys. Lett. B* **603**, 1 (2004) [arXiv:hep-th/0403127]; R. G. Cai, *Phys. Lett. B* **657**, 228 (2007) [arXiv:0707.4049 [hep-th]]; H. Wei and R. G. Cai, *Phys. Lett. B* **660**, 113 (2008) [arXiv:0708.0884 [astro-ph]]. B. Feng, X. L. Wang and X. M. Zhang, *Phys. Lett. B* **607**, 35 (2005) [arXiv:astro-ph/0404224]; C. Gao, X. Chen and Y. G. Shen, *Phys. Rev. D* **79**, 043511 (2009) [arXiv:0712.1394 [astro-ph]].
- [7] D. Huterer and M. S. Turner, *Phys. Rev. D* **64**, 123527 (2001) [arXiv:astro-ph/0012510]; A. R. Cooray and D. Huterer, *Astrophys. J.* **513**, L95 (1999) [arXiv:astro-ph/9901097]; D. Huterer and M. S. Turner, *Phys. Rev. D* **60**, 081301 (1999) [arXiv:astro-ph/9808133]; J. Weller and A. J. Albrecht, *Phys. Rev. Lett.* **86**, 1939 (2001) [arXiv:astro-ph/0008314].
- [8] M. Chevallier and D. Polarski, *Int. J. Mod. Phys. D* **10**, 213 (2001) [arXiv:gr-qc/0009008].
- [9] E. V. Linder, *Phys. Rev. Lett.* **90**, 091301 (2003) [arXiv:astro-ph/0208512].
- [10] D. Huterer and G. Starkman, *Phys. Rev. Lett.* **90**, 031301 (2003) [arXiv:astro-ph/0207517].
- [11] D. Huterer and A. Cooray, *Phys. Rev. D* **71**, 023506 (2005) [arXiv:astro-ph/0404062].
- [12] A. Hojjati, L. Pogosian and G. B. Zhao, arXiv:0912.4843 [astro-ph.CO].
- [13] Y. Wang, *Phys. Rev. D* **80**, 123525 (2009) [arXiv:0910.2492 [astro-ph.CO]].
- [14] S. Sullivan, A. Cooray and D. E. Holz, *JCAP* **0709**, 004 (2007) [arXiv:0706.3730 [astro-ph]].
- [15] G. B. Zhao, D. Huterer and X. Zhang, *Phys. Rev. D* **77**, 121302 (2008) [arXiv:0712.2277 [astro-ph]].

- [16] P. Serra, A. Cooray, D. E. Holz, A. Melchiorri, S. Pandolfi and D. Sarkar, arXiv:0908.3186 [astro-ph.CO].
- [17] Y. Gong, R. G. Cai, Y. Chen and Z. H. Zhu, arXiv:0909.0596 [astro-ph.CO].
- [18] M. Hicken *et al.*, *Astrophys. J.* **700**, 331 (2009) [arXiv:0901.4787 [astro-ph.CO]].
- [19] W. J. Percival *et al.*, arXiv:0907.1660 [astro-ph.CO].
- [20] E. Komatsu *et al.* [WMAP Collaboration], *Astrophys. J. Suppl.* **180**, 330 (2009) [arXiv:0803.0547 [astro-ph]].
- [21] J. Simon, L. Verde and R. Jimenez, *Phys. Rev. D* **71**, 123001 (2005) [arXiv:astro-ph/0412269].
- [22] E. Gaztanaga, A. Cabre and L. Hui, arXiv:0807.3551 [astro-ph].
- [23] A. J. S. Hamilton and M. Tegmark, *Mon. Not. Roy. Astron. Soc.* **312**, 285 (2000) [arXiv:astro-ph/9905192].
- [24] R. de Putter and E. V. Linder, *Astropart. Phys.* **29**, 424 (2008) [arXiv:0710.0373 [astro-ph]].
- [25] S. Nesseris and L. Perivolaropoulos, *Phys. Rev. D* **72**, 123519 (2005) [arXiv:astro-ph/0511040].
- [26] D. J. Eisenstein and W. Hu, *Astrophys. J.* **496**, 605 (1998) [arXiv:astro-ph/9709112].
- [27] Q. G. Huang, M. Li, X. D. Li and S. Wang, *Phys. Rev. D* **80**, 083515 (2009) [arXiv:0905.0797 [astro-ph.CO]]; G. B. Zhao and X. Zhang, arXiv:0908.1568 [astro-ph.CO]; S. Qi, T. Lu and F. Y. Wang, arXiv:0904.2832 [astro-ph.CO].
- [28] W. Hu and N. Sugiyama, *Astrophys. J.* **471**, 542 (1996) [arXiv:astro-ph/9510117].
- [29] H. Zhang, arXiv:0909.3013 [astro-ph.CO].
- [30] R. Lazkoz, S. Nesseris and L. Perivolaropoulos, *JCAP* **0511**, 010 (2005) [arXiv:astro-ph/0503230]; M. X. Luo and Q. P. Su, *Phys. Lett. B* **626**, 7 (2005) [arXiv:astro-ph/0506093].
- [31] In preparing.
- [32] J. C. B. Sanchez, S. Nesseris and L. Perivolaropoulos, *JCAP* **0911**, 029 (2009) [arXiv:0908.2636 [astro-ph.CO]]; H. Wei, arXiv:0906.0828 [astro-ph.CO]; Y. Gong, B. Wang and R. G. Cai, arXiv:1001.0807 [astro-ph.CO].
- [33] D. J. Eisenstein *et al.* [SDSS Collaboration], *Astrophys. J.* **633**, 560 (2005) [arXiv:astro-ph/0501171].
- [34] J. H. He, B. Wang and P. Zhang, *Phys. Rev. D* **80**, 063530 (2009) [arXiv:0906.0677 [gr-qc]]; R. G. Cai and Q. Su, arXiv:0912.1943 [astro-ph.CO]; C. Feng, B. Wang, E. Abdalla and R. K. Su, *Phys. Lett. B* **665**, 111 (2008) [arXiv:0804.0110 [astro-ph]]; H. H. Xiong, Y. F. Cai,



T. Qiu, Y. S. Piao and X. Zhang, Phys. Lett. B **666**, 212 (2008) [arXiv:0805.0413 [astro-ph]].